Design of a Ropeless Elevator with Linear Induction Motor taking into account Edge and end effects

M. Abd El-Moaty Zaher, M. Kamal Ahmed and M. Shafik Abd El-Razek

Electrical Power and Machines Department, Faculty of Engineering, Al-Azhar University, Cairo, Egypt.
Msh.egypt@yahoo.com

Abstract: The aim of this paper is to present a novel elevator drive's system for high rise building, this elevator is based on single-sided linear induction motor (SLIM). The main article is studies the design of SLIM using a user-interactive MATLAB program. Our goal of this work was the development of an elevator system with reducing the required space of elevator hoist-ways in high rise buildings and to achieve higher speed at more economic operation. The equivalent circuit model of the SLIM was studied with choosing various design parameters to obtain the performance as well as thrust and efficiency. This paper describes the various effects of LIM and compares SLIM performance with and without transverse edge and end effects.

[M. Abd El-Moaty Zaher, M. Kamal Ahmed and M. Shafik Abd El-Razek. **Design of a Ropeless Elevator with Linear Induction Motor taking into account Edge and end effects.** J Am Sci 2012;8(5):505-517]. (ISSN: 1545-1003). http://www.americanscience.org. 53

Keywords: Elevator, single-sided linear induction motor.

1. Introduction

Great effort had been done to enhancement the performance elevators drives without counter weight. Due to an increasing travel height the handling capacity will be reduced, in consequence that for the upper areas of high rise buildings more and more elevators are required. Limits of these elevator layouts are costly and the needed large hoist-way areas at the entrance level. Due to an existing high rise building, these new elevator systems will be described and compared with the realized and designed today usual systems, the comfort is higher at high rise buildings, where all floors are reachable from ground floor without transfer. Furthermore, the rope is mostly steel wire and causes control problems for the much higher building due to its mass and vertical vibration and so on. In this respect, linear electric motors are suitable for the vertical applications with less limitation on height of building and space occupancy. Below some advantages and disadvantages are presented. The major inherent advantages of ropeless elevator with SLIM over Traditional Technologies [1-4].

- Absence of a machine room.
- Absence of traction equipment.
- Hoist-way is smaller due to the absence of a counter weight.
- Zero backlash at higher accuracy.
- High acceleration and velocity reduces cycle times
- High accuracy and repeatability provides better quality control
- Exact positioning in closed loop systems.
- All electro-mechanical controlled systems used for an induction motors can be adopted for a LIM without any bigger changes.
- Economical and cheap maintenance.

2. Structure of the (slim)

In practice, the primary or stator of a LIM consists of a rectangular slotted structure formed by a stack of steel laminations. Within the slots of the primary stack are laid the polyphase windings to produce the linearly traveling magnetic field, just like the rotating magnetic field in a rotary induction motor, produced by the polyphase stator windings. The secondary of the LIM, or rotor, which is an aluminum sheet (or copper), with or without a solid back iron plate, completes the magnetic circuit and creates the magnetic flux linkage across the air gap. This in turn induces a voltage on the conductive wall, which generates an eddy current in the conducting outer layer of the secondary. The interaction between the eddy current and the changing electromagnetic field generates electromagnetic thrust on the plate in the longitudinal direction of the motor. A single-sided short primary LIM is shown in Fig. 1, [5].

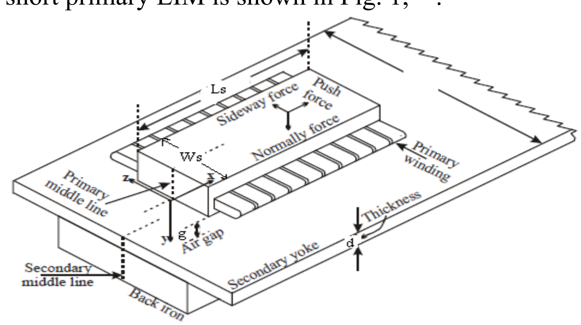

Figure 1. Geometry of single-sided linear induction motor

3. Design of The Slim for Rope less Elevator

For the analysis and design of a SLIM, an approximate equivalent circuit will be used. To determine the parameters of the circuit, the design formulas of the rotary induction motor for application will be adapted to the SLIM. As known, often the secondary of a LIM is made of a conducting sheet. The concept of surface resistivity is very useful in finding the resistance of such a secondary. The approximate equivalent circuit is on a per phase basis of a LIM is presented as shown in Fig. 2. The core losses are neglected because a realistic air gap flux density leads to moderate flux densities in the core and hence, rather low core losses. Skin effect is small at rated frequency for a flat linear induction motor with a thin conductive sheet on the secondary, therefore equivalent secondary inductance is negligible [6, 7]. The remaining non-negligible parameters are shown in Fig 2 and are discussed below.

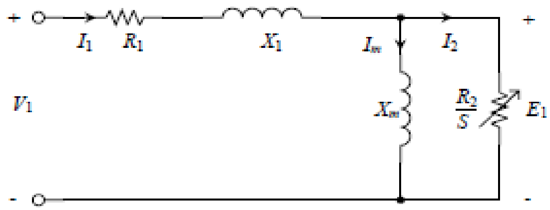

Figure 2. Equivalent circuit of a per-phase SLIM.

Considering the edge effects, the equivalent circuit parameters of a SLIM can be written as follows [8-10]:

$$R_1 = \frac{\rho_w (2W_s + 2l_{ce}) J_1 N_1}{I_1} \quad (1)$$

$$X_1 = \frac{8\mu_o \pi f [(\lambda_s (1 + \frac{3}{p}) + \lambda_d) \frac{W_s}{q_1} + \lambda_e l_{ce}] N_1^2}{p} \quad (2)$$

Where: R_1 is primary phase resistance and X_1 is leakage reactance.

The magnetizing reactance;

$$X_m = \frac{24 \mu_o \pi f W_s K_w N_1^2 \tau}{\pi^2 p g_{ei}} \quad (3)$$

The goodness factor is now given by;

$$G = \frac{2\mu_o f \tau^2}{\pi (\frac{\rho_r}{d}) g_{ei}} \quad (4)$$

The secondary resistance; $R_2 = \frac{X_m}{G_{ei}}$ (5)

Performance of a LIM (whose equivalent circuit parameters are known and iron losses, additional losses produced by harmonics are neglected) can be calculated as follows [8-10]:

Input power; $P_i = m V_1 I_1 \cos\varphi$ (6)

The secondary phase current; $I_2 = \frac{I_1}{\sqrt{(\frac{1}{(SG)^2} + 1)}}$ (7)

The input power to the stator windings is utilized in producing useful mechanical power which is exerted on the rotor and to account for the rotor copper losses. In terms of the equivalent circuit components, the mechanical power developed by the rotor is the power transferred across the air-gap from the stator to the rotor $(mI_2^2 \frac{R_2}{S})$ minus the rotor copper $(mI_2^2 R_2)$;

$$P_o = m I_2^2 R_2 (\frac{1-S}{S}) \quad (8)$$

The total mechanical power developed by the rotor of the SLIM is given by; $P_o = F_s V_r$ (9)

The SLIM efficiency; $\eta = \frac{P_o}{P_i}$ (10)

The total thrust Fs may be written as;

$$F_s = \frac{m I_1^2 R_2}{2\pi f S[(\frac{1}{SG_{ei}})^2 + 1]} \quad (11)$$

Neglecting the iron losses, the efficiency and power factor are;

$$\eta = \frac{F_s 2\tau f (1-S)}{F_s 2\tau f + m I_1^2 R_1} \quad (12)$$

$$\cos\varphi = \frac{F_s 2\tau f + m I_1^2 R_1}{m V_1 I_1} \quad (13)$$

In reality there are quite a few differences between linear and rotary IM's such as the magnetic circuit is open at the two longitudinal ends (along the traveling field direction). As the flux law has to be observed, the air gap field will contain additional waves whose negative influence on performance is called dynamic longitudinal end effect according to figure (3a). In short primaries (with 2, 4 poles), there are current asymmetries between phases due to the fact that one phase has a position to the core longitudinal ends which is different from those of the other two. This is called static longitudinal effect according to figure (3b). Due to same limited primary core length, the back iron flux density tends to include an additional non traveling (ac) component which should be considered when sizing the back iron of LIM's according to figure (3c). In the SLIM, there is only one primary along one side of secondary), there is a normal force (of attraction or repulsion type) between the primary and secondary. This normal force may be put to use to compensate for part of the weight of the moving primary and thus reduce the wheel wearing and noise level according to figure (3d). For secondaries with aluminum (copper) sheet with (without) solid back iron, the induced currents have part of their closed paths contained in the active (primary core) zone. They have additional-longitudinal (along OX axis)-components which produce additional losses in the secondary and a distortion in the air gap flux density along the transverse direction (OY). This is called the transverse edge effect. When the primary is placed off center along OY, the longitudinal components of the current density in the active zone produce an ejection type lateral force. At the same time, the secondary back core tends to realign the primary along OY. So the resultant lateral force may be either decentralizing or centralizing in character according to figure (3f). All these differences between linear and rotary IM's warrant a specialized investigation of field distribution and performance in order to limit the adverse effects (longitudinal end effects and back iron flux distortion, etc.) and exploit the desirable ones (normal and lateral forces, or transverse edge effects) [11, 12].

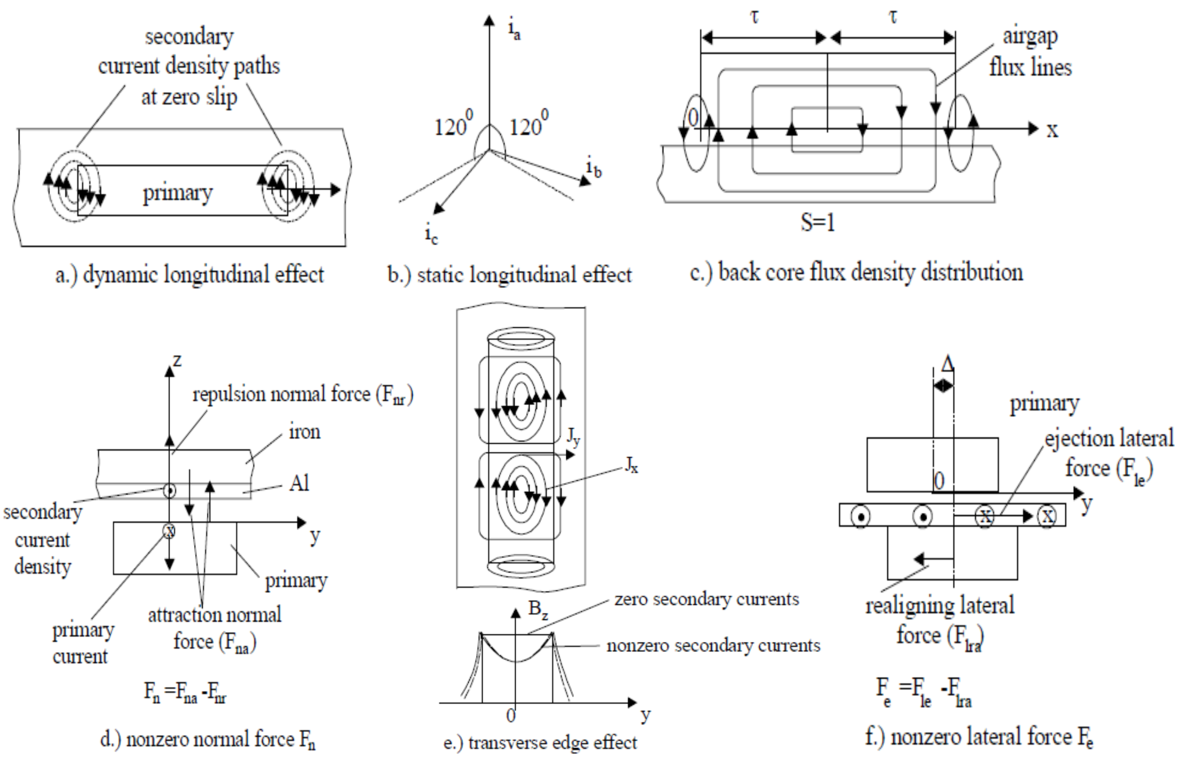

Figure 3. Panoramic view of (LIM).

A simplified single dimensional theory of transverse edge effect is presented here. Due to this, transverse and longitudinal components of current densities exist, consequently increasing the secondary resistance R_2 by a multiplicative factor K_t, and a reducing the magnetizing reactance by a multiplicative factor K_m.

$$K_t = \frac{k_x^2}{k_r} \frac{1 + (\frac{SGk_r}{k_x})^2}{1 + S^2 G^2} \geq 1 \tag{14}$$

$$K_m = \frac{k_r}{k_r} K_t \leq 1 \tag{15}$$

The stator slotting is considered only through Carter coefficient K_c.

$$K_c = \frac{\lambda}{\lambda - \gamma g_o} \tag{16}$$

The skin effect coefficient for aluminum is neglected or considered through the standard correction coefficient.

$$K_{sk} = \frac{d}{d_s}\left[\frac{\sinh(\frac{2d}{d_s}) + \sin(\frac{2d}{d_s})}{\cosh(\frac{2d}{d_s}) - \cos(\frac{2d}{d_s})}\right] \tag{17}$$

For a large air gap, there is a kind of flux leakage

$$K_{leakage} = \frac{\sinh(\frac{g}{2\tau})}{\frac{g}{2\tau}} > 1 \tag{18}$$

There are no overhangs for secondary back iron $c = \frac{W_s}{2}$ the transverse edge effect coefficient K_t

$$K_{ti} = \frac{1}{1 - \frac{2\tau}{\pi W_s}\tanh(\frac{\pi W_s}{2\tau})} \tag{19}$$

The depth of field penetration in the secondary back iron δ_i is thus

$$\delta_i = real\left(\frac{1}{(\frac{\pi^2}{\tau^2} + j2\pi f \mu_i \frac{S\sigma_i}{K_{ti}})^{1/2}}\right) \tag{20}$$

In a similar way an equivalent air gap may be defined which accounts for the magnetic path in the secondary path by a coefficient K_p

$$K_p = \frac{\tau^2 \mu_0}{2\pi^2 g K_c \delta_i \mu_i} \tag{21}$$

$$g_e = (1 + K_p) g \frac{K_c K_{leakage}}{K_m} \tag{22}$$

Now the equivalent goodness factor G may be written as

$$G = \frac{2\mu_0 f \tau^2 d}{\pi g_e \rho_r} \tag{23}$$

The end effect force at zero slip may be either propulsive positive for low goodness factor values or (and) large number of poles or it may be of braking character negative for high goodness factor or (and) smaller number of poles. For a given number of poles and zero slip, there is a certain value of the realistic goodness factor, for which the end effect force is zero [11, 12]. This value of goodness factor is called the optimum goodness factor. The existence of the end effect force at zero slip is a distinct manifestation of longitudinal end effect. Per unit end effect force $F_{xe(pu)}$

$$F_{xe(pu)} = F_{xe} \frac{\pi^2 g_e}{\frac{W_s}{2} \mu_o J_m} \tag{24}$$

$$F_{xe} = real\left[B_t \frac{-1 + \exp(p\tau(\gamma_2 - j\frac{\pi}{\tau}))}{\gamma_2 - j\frac{\pi}{\tau}}\right] \tag{25}$$

$$B_t = j\frac{J_m}{D}(\gamma_1 \frac{\tau}{\pi} + SG) \tag{26}$$

$$D = g_e(\gamma_2 - \gamma_1)(1 + jSG) \tag{27}$$

$$\gamma_{1,2} = \pm \frac{a_1}{2}\left[\sqrt{\frac{b1+1}{2}} \pm 1 + j\sqrt{\frac{b_1 - 1}{2}}\right] \tag{28}$$

$$a_1 = \frac{\pi}{\tau} G(1 - S) \tag{29}$$

$$b_1 = \sqrt{1 + \left(\frac{4}{G(1-S)^2}\right)^2} \tag{30}$$

Where (B_t, D, a_1, b_1) are constants and (γ_1, γ_2) called roots of the characteristic equation.
The end effect influence may be written as;

$$f_e = \frac{1 + S^2G^2}{SG} real\left[\frac{j\left(\frac{\gamma_1 \tau}{\pi} + SG\right)\left(\exp\left(p\tau\left(\gamma_2 \frac{\tau}{\pi}\right)\right) - 1\right)}{\frac{\tau}{\pi}(\gamma_2 - \gamma_1)(1 - jSG)p\pi\left(\gamma_2 \frac{\tau}{\pi} - j\right)}\right] \tag{31}$$

4.Flow Chart for The Design of Slim-Ropeless Elevator

This is the complete procedure for the design of a ropeless elevator with SLIM using a user interactive computer program, for which the flow chart is as shown in Fig. 4. This program allows the user to choose a variety of desired values in the design of SLIM unit like the desired SLIM thrust, rotor velocity, rated slip and many other design parameters. The SLIM-ropeless elevator is designed according to the following flow chart.

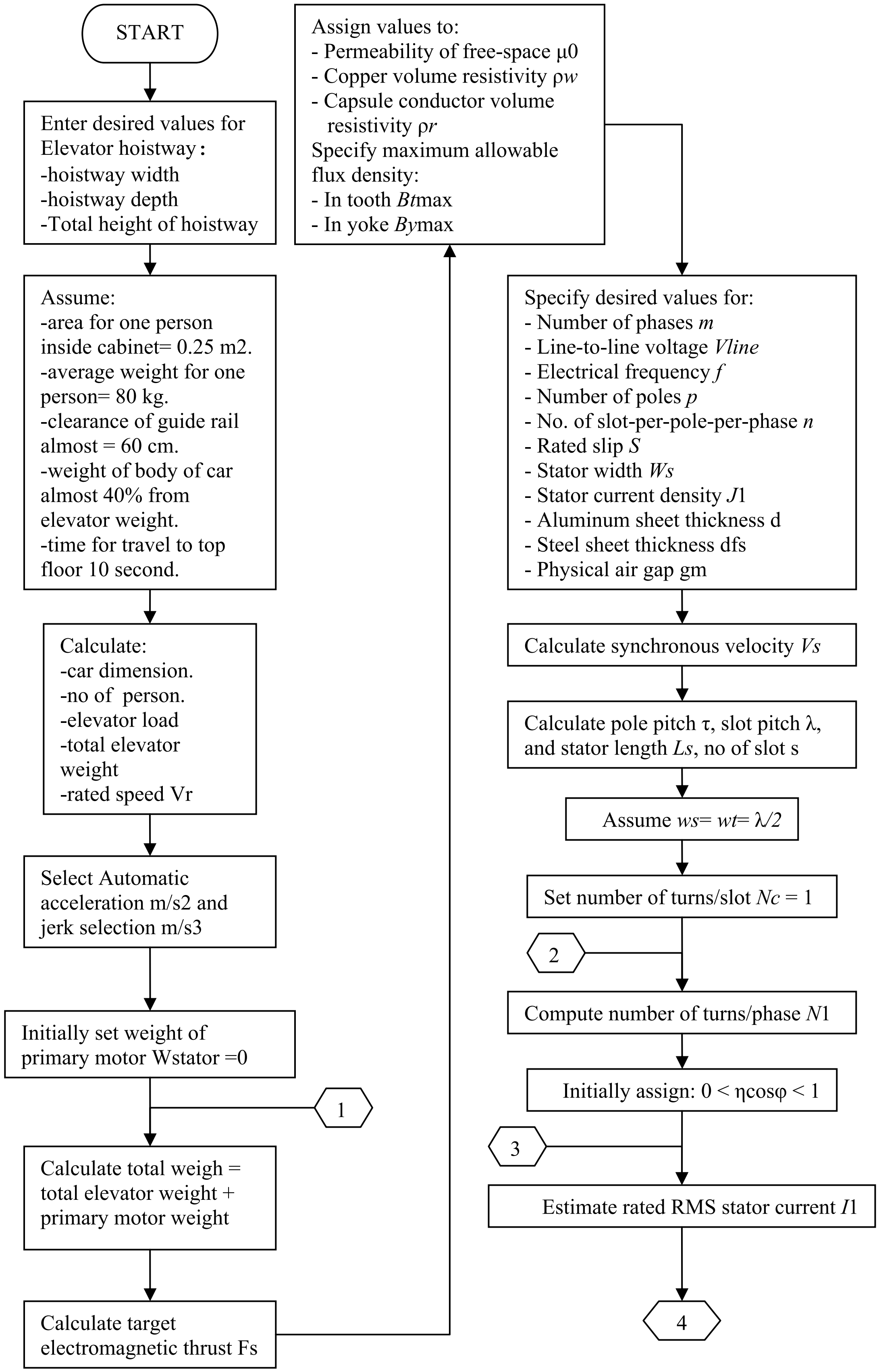
START
Enter desired values for Elevator hoistway :
-hoistway width
-hoistway depth
-Total height of hoistway
Assume:
-area for one person inside cabinet= 0.25 m2.
-average weight for one person= 80 kg.
-clearance of guide rail almost = 60 cm.
-weight of body of car almost 40% from elevator weight.
-time for travel to top floor 10 second.
Calculate:
-car dimension.
-no of person.
-elevator load
-total elevator weight
-rated speed Vr
Select Automatic acceleration m/s2 and jerk selection m/s3
Initially set weight of primary motor Wstator =0
1
Calculate total weigh = total elevator weight + primary motor weight
Calculate target electromagnetic thrust Fs
Assign values to:
- Permeability of free-space μ0
- Copper volume resistivity ρw
- Capsule conductor volume resistivity ρr
Specify maximum allowable flux density:
- In tooth Btmax
- In yoke Bymax
Specify desired values for:
- Number of phases m
- Line-to-line voltage Vline
- Electrical frequency f
- Number of poles p
- No. of slot-per-pole-per-phase n
- Rated slip S
- Stator width Ws
- Stator current density J1
- Aluminum sheet thickness d
- Steel sheet thickness dfs
- Physical air gap gm
Calculate synchronous velocity Vs
Calculate pole pitch τ, slot pitch λ, and stator length Ls, no of slot s
Assume ws= wt= λ/2
Set number of turns/slot Nc = 1
2
Compute number of turns/phase N1
Initially assign: 0 < ηcosφ < 1
3
Estimate rated RMS stator current I1
4

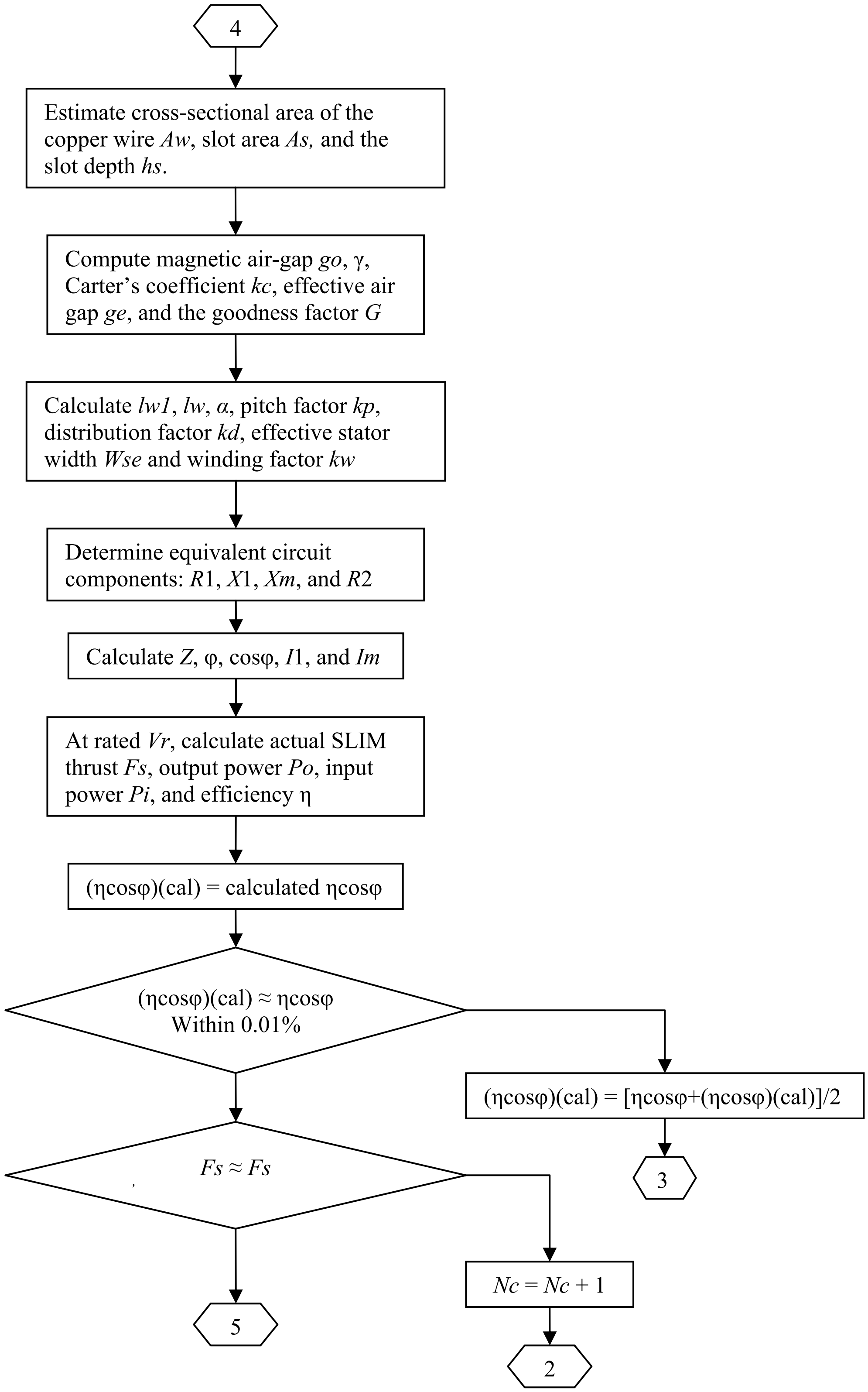
4
Estimate cross-sectional area of the copper wire Aw, slot area As, and the slot depth hs.
Compute magnetic air-gap go, γ, Carter's coefficient kc, effective air gap ge, and the goodness factor G
Calculate lw1, lw, α, pitch factor kp, distribution factor kd, effective stator width Wse and winding factor kw
Determine equivalent circuit components: R1, X1, Xm, and R2
Calculate Z, φ, cosφ, I1, and Im
At rated Vr, calculate actual SLIM thrust Fs, output power Po, input power Pi, and efficiency η
(ηcosφ)(cal) = calculated ηcosφ
(ηcosφ)(cal) ≈ ηcosφ Within 0.01%
(ηcosφ)(cal) = [ηcosφ+(ηcosφ)(cal)]/2
3
Fs ≈ Fs
Nc = Nc + 1
5
2

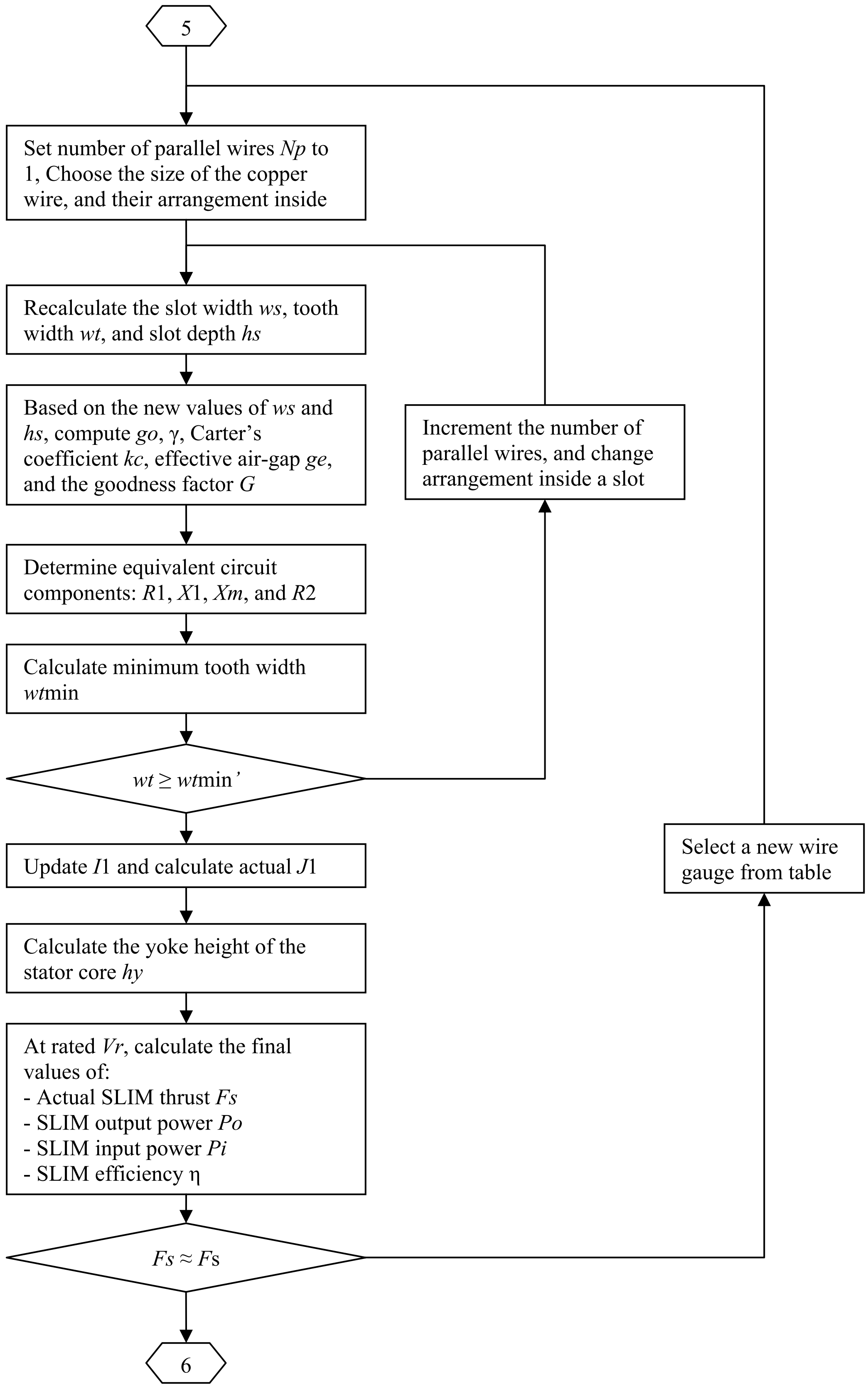
5
Set number of parallel wires Np to 1, Choose the size of the copper wire, and their arrangement inside
Recalculate the slot width ws, tooth width wt, and slot depth hs
Based on the new values of ws and hs, compute go, γ, Carter's coefficient kc, effective air-gap ge, and the goodness factor G
Increment the number of parallel wires, and change arrangement inside a slot
Determine equivalent circuit components: R1, X1, Xm, and R2
Calculate minimum tooth width wtmin
wt ≥ wtmin'
Update I1 and calculate actual J1
Select a new wire gauge from table
Calculate the yoke height of the stator core hy
At rated Vr, calculate the final values of:
- Actual SLIM thrust Fs
- SLIM output power Po
- SLIM input power Pi
- SLIM efficiency η
Fs ≈ Fs
6

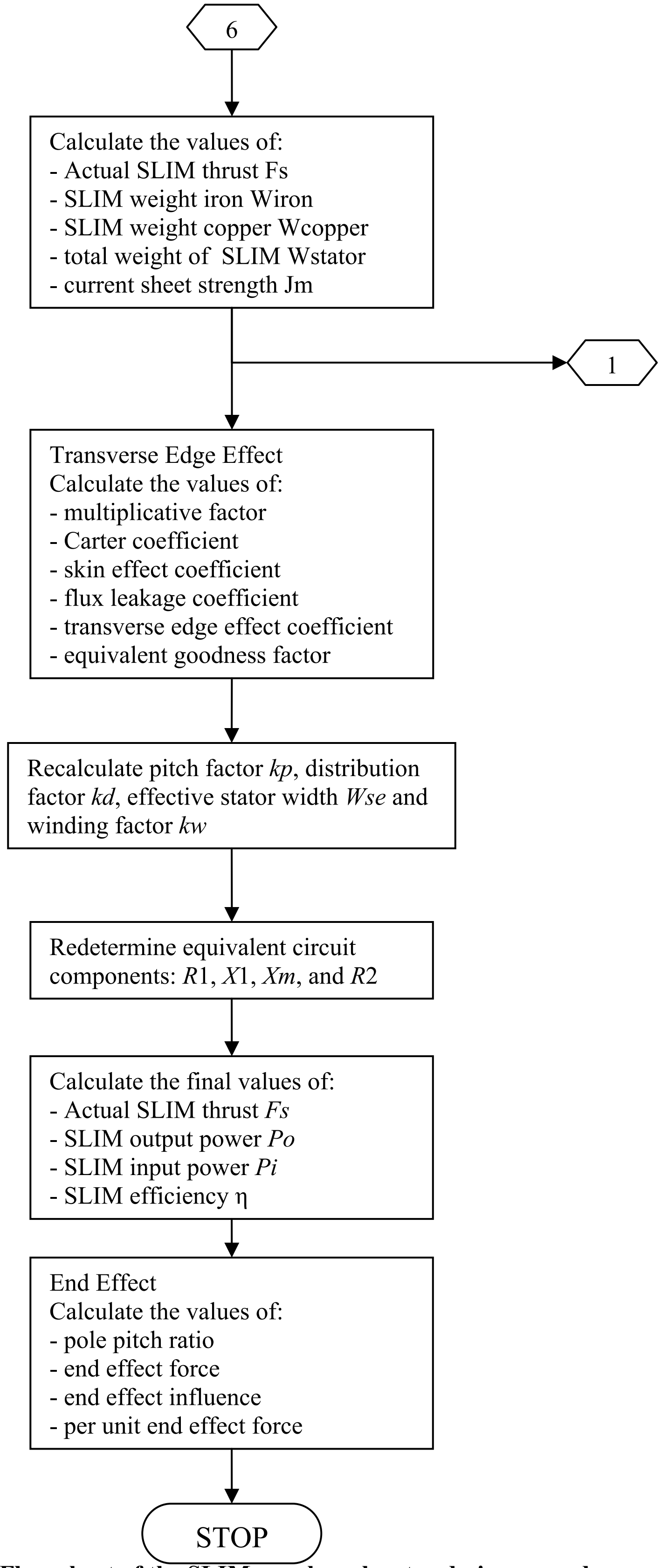

Figure 4. Flow chart of the SLIM-ropeless elevator design procedure.

5. Characteristic Curves of Slim

The SLIM designs for a rated rotor velocity of 20 m/s, a target thrust of 4916N at slips of 10%. Once the design parameters were obtained, the performance of the SLIM stator as a function of rotor velocity, are evaluated as shown in the following figures. The performance curves of the SLIM with and without transverse edge effect, thrust Fs and efficiency η as a function of rotor velocity Vr are as shown in Figs. 5, 6.

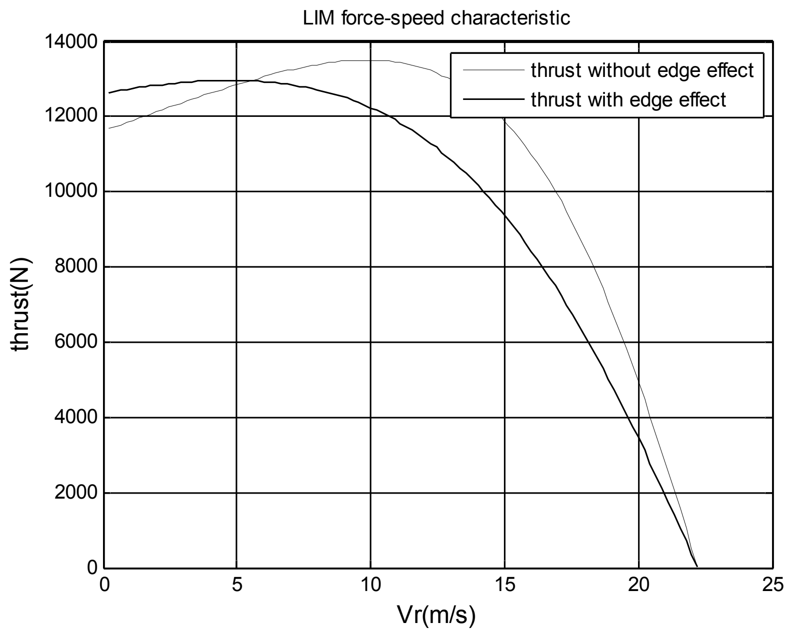

Figure 5. Thrust Fs versus rotor velocity Vr of one SLIM stator unit with and without edge effect at a rated slip of 10% for elevator hoistway dimension (width 3m, depth 3m, total height 400m)

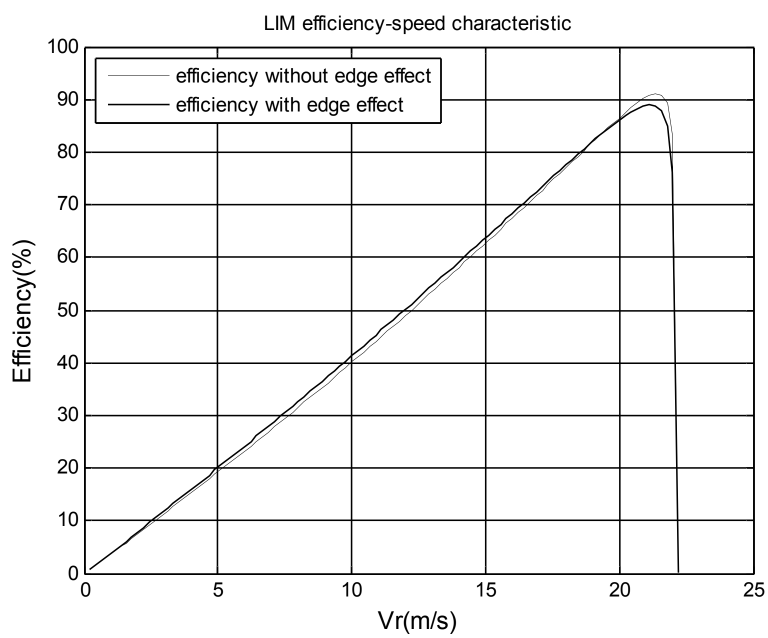

Figure 6. Efficiency η versus rotor velocity Vr of one SLIM stator unit with and without edge effect at a rated slip of 10% for elevator hoistway dimension (width 3m, depth 3m, total height 400m)

The main consequences of transverse edge effects appear in the forms of an increase in secondary resistivity, a reducing the magnetizing reactance, increase start force, reduce efficiency, tendency toward lateral instability, distortion of air gap fields, and deterioration of the LIM performance. This effect can be neglected in our calculation as well as our mathematical model of SLIM. The end effect force at zero slip may be either propulsive positive for low goodness factor values or (and) large number of poles or it may be of braking character negative for high goodness factor or (and) smaller number of poles. The effect of backward (exit) end effect wave is negligible. The forward (entry) end effect wave which attenuates slowly in the air gap along the direction of motion. The higher the value of goodness factor and the lower the slip, the more important the end effect waves are. End effect force as a function of slip is as shown in Fig. 7.

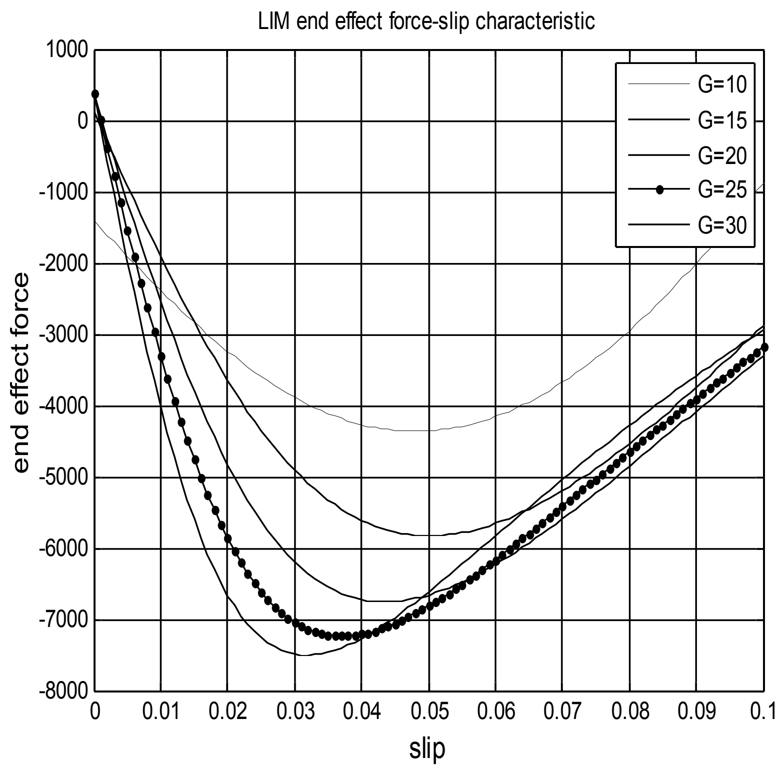

Figure 7. relative end effect force versus slip of one SLIM stator unit with edge effect for elevator hoistway dimension (width 3m, depth 3m, total height 400m), Effect of goodness factor on the plot.

6. Evaluation of Performance of Slim by Changing Parameters

The performance of the SLIM based on this particular design is evaluated by varying certain parameters like the thickness of secondary, mechanical air-gap and the number of poles. Based on this evaluation, the best possible values for these parameters are selected as shown in the sections below.

6.1 Effect of Aluminum thickness on the performance parameters

The effect of varying the thickness of the aluminum sheet on the rotor of SLIM on its performance, from 0.3mm to 4.3mm in steps of 1mm is as shown in Figs. 8, 9. The thickness of aluminum sheet on the rotor, d, plays a significant role in the performance, the thicker the secondary, the larger the goodness factor. Also, thicker aluminum sheet will increase the magnetic air-gap. As the thickness of Aluminum sheet is increased the magnitude of thrust also increases. But, as stated before, as the thickness of secondary sheet is increased the magnetic air-gap also increases which causes the magnitude of thrust to decrease. The efficiency does not have significant impact with an increase in aluminum thickness. It can be seen that various aluminum thicknesses have the same efficiency at the rated rotor velocity.

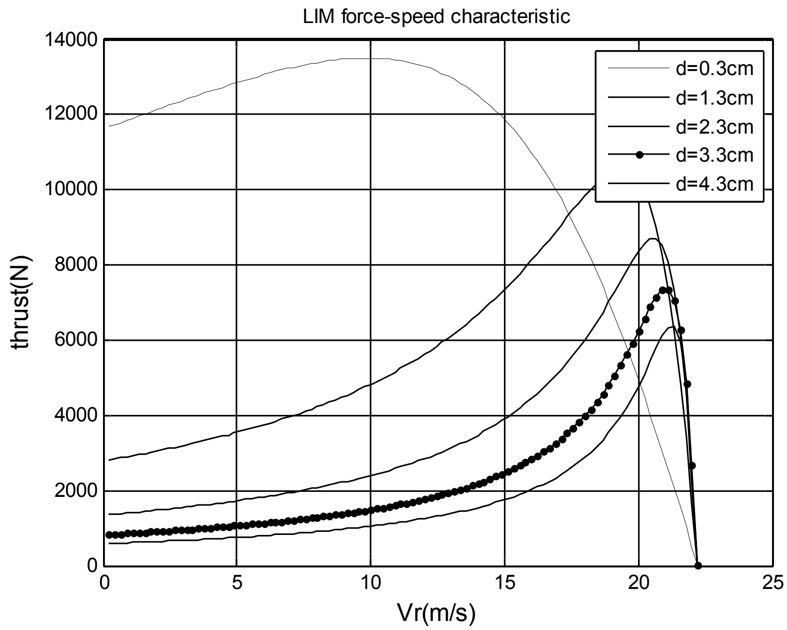

Figure 8. Effect of aluminum thickness on the thrust of SLIM plotted against rotor velocity

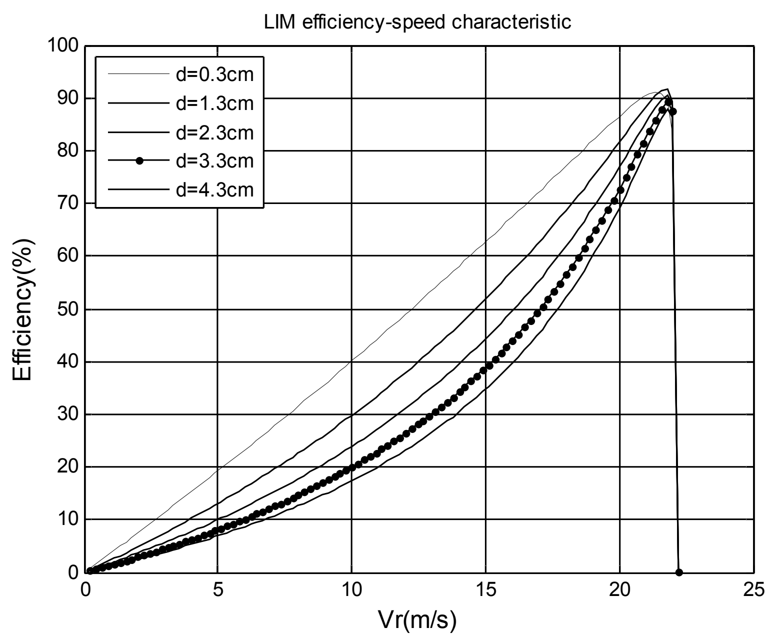

Figure 9. Effect of aluminum thickness on efficiency of SLIM plotted against rotor velocity

6.2 Effect of Mechanical air-gap on performance

The length of the air gap is very important parameter in machine design. A large air gap requires a large magnetizing current and results in a smaller power factor. In the case of an SLIM, exit-end zone losses increase with a larger air gap. Also, output force and efficiency decrease when the design incorporates a large air gap. The goodness factor is inversely proportional to the air gap. Thus, it is clear that the air gap should be as small as is mechanically possible. The different performance values with varying air-gap are shown in Figs. 10, 11. When the air-gap is changed from 1 cm to 5 cm, keeping all other parameters fixed, the efficiency decreases with increasing air-gap and the stand still thrust decreases as the air-gap is increased.

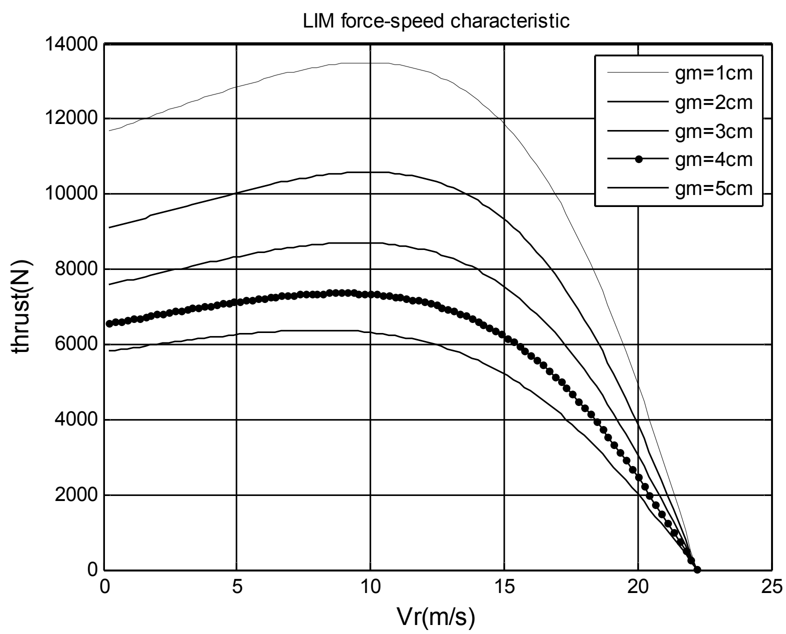

Figure 10. Effect of mechanical air-gap on the thrust of SLIM plotted against rotor velocity

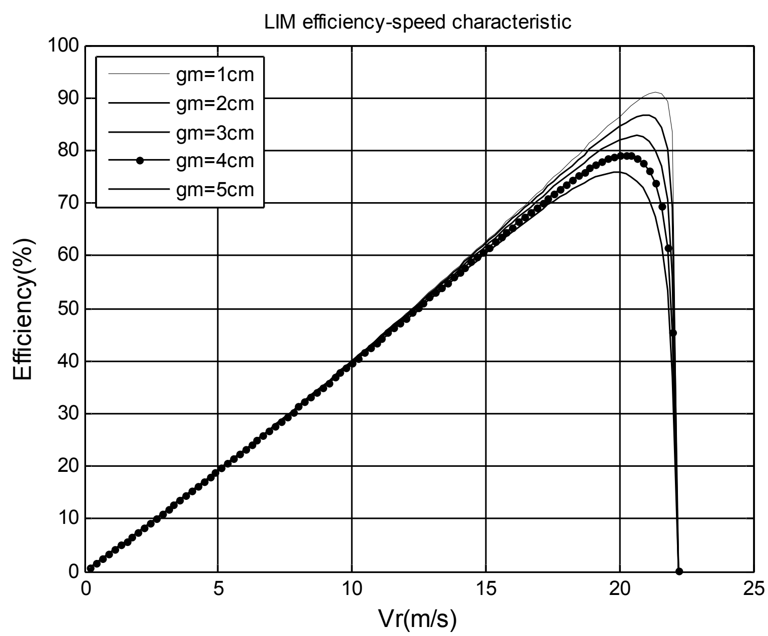

Figure 11. Effect of mechanical air-gap on efficiency of SLIM plotted against rotor velocity

7.Conclusion

A ropeless elevator with single-sided linear induction motor (SLIM) drive system has been explored and validated as an alternative linear vertical transverse in this paper. We can conclude that the transverse edge effects can be neglected. The end effect force at zero slip may be either propulsive positive for low goodness factor values or (and) large number of poles or it may be of braking character negative for high goodness factor or (and) smaller number of poles. We can conclude that the air-gap plays a very important role in the performance of the SLIM. Care should be taken in choosing these parameters. Based on our target values of rotor velocity and thrust, these parameters should be chosen which gives the best possible thrust closest to the target value at a decent value of efficiency.

References

1. Ishii T. (1994): "Elevators for skyscrapers", IEEE Spectrum, vol. 31, pp.: 42-46, September.

2. Hans M. Jappsen, Günther Stangier (…..), "High rise elevators for the 21st century", http://jappseningenieure.de/daten/downloads/en/6_en.pdf.
3. Stein, Benjamin, Reynolds, John S., Grondzik, Walter T., and Alison G. Kwok, (2006): "Mechanical and Electrical Equipment for Buildings" 10th ed. Hoboken, New Jersey: John Wiley and Sons, Inc.
4. Roma Rinkeviciene, Saulius Lisauskas, Vygintas Batkauskas(2007): "Application and analysis of linear induction motors in mechatronic systems", Doctoral school of energy and geo-technology. Vilnius Gediminas Technical University.
5. Fevzi kentli, Ismail kiyak, Nevzat onat (2005): " an example for design and application of low-speed linear induction motor (LIM)", Marmara University, Faculty of Technical Education, Department of Electrical Education,, Istanbul, Turkey, eleco'2005 4 th international conference. www.emo.org.tr/ekler/96f4710c33a97fd_ek.pdf.
6. Robert O'Connell, Sarveswara Bhamidi (2005): "Design of a single sided linear induction motor using a user interactive computer program", Thesis (M.S.) University of Missouri-Columbia.
7. Pai, R.M.; Boldea, I.; Nasar, S.A. (1988): "A complete equivalent circuit of a linear induction motor with sheet secondary", IEEE Transactions on , vol: 24 , Issue(1) , pp.: 639-654 , Jan. .
8. Nasar, S.A. and Boldea, I. (1987): "Linear Electric Motors", Prentice-Hall, Inc., Englewood Cliffs, New Jersey.
9. Nasar S. A., I. Boldea(1976): "Linear Motion Electric Machines", John Wiley & Sons Inc., New York.
10. Wisuwat Plodpradistha (2002): "Study of Tubular Linear Induction Motor for Pneumatic Capsule Pipeline system", Ph.D. Dissertation, Department of Electrical Engineering, University of Missouri- Columbia, May.
11. Ion Boldea and Syed Nasar (2002):"The Induction Machine Handbook",.
12. Bhag S. Guru and Huseyin R. Hiziroglu (2001): "Electric Machinery and Transformers", oxford university press, New York,.
13. Budig P.-K. (2000): "The application of linear motors" in Proc. 3rd IEEE Int. Power Electronics and Motion Control Conf., vol.3, pp.: 1336 – 1341, August.
14. I Boldea. and S. A.Nasar (2001):"Linear Motion Electromagnetic Devices" USA, Taylor & Francis.

4/29/2012